# Cross-correlation frequency resolved optical gating analysis of broadband continuum generation in photonic crystal fiber: simulations and experiments

**John M. Dudley**
*Laboratoire d'Optique P. M. Duffieux, Université de Franche-Comté, 25030 Besançon, France*
*john.dudley@univ-fcomte.fr*

**Xun Gu, Lin Xu, Mark Kimmel, Erik Zeek, Patrick O'Shea, Rick Trebino**
*School of Physics, Georgia Institute of Technology, Atlanta, GA 30332-0430, USA*

**Stéphane Coen**
*Service d'Optique et Acoustique, Université Libre de Bruxelles, Av. F. D. Roosevelt 50, CP 194/5, B-1050 Brussels, Belgium*

**Robert S. Windeler**
*OFS Fitel Laboratories, 700 Mountain Ave., Murray Hill, NJ 07974, USA*

**Abstract:** Numerical simulations are used to study the temporal and spectral characteristics of broadband supercontinua generated in photonic crystal fiber. In particular, the simulations are used to follow the evolution with propagation distance of the temporal intensity, the spectrum, and the cross-correlation frequency resolved optical gating (XFROG) trace. The simulations allow several important physical processes responsible for supercontinuum generation to be identified and, moreover, illustrate how the XFROG trace provides an intuitive means of interpreting correlated temporal and spectral features of the supercontinuum. Good qualitative agreement with preliminary XFROG measurements is observed.



**OCIS codes:** (320.0320) Ultrafast optics (190.4370) Nonlinear optics, fibers; (999.999) Microstructure fibers, (999.999) Photonic crystal fibers

## References and links

1. J. K. Ranka, R. S. Windeler, A. J. Stentz, " Visible continuum generation in air-silica microstructure optical fibers with anomalous dispersion at 800 nm" Opt. Lett. **25**, 25-27 (2000).
2. J. H. V. Price, W. Belardi, T. M. Monro, A. Malinowski, A. Piper, D. J. Richardson, "Soliton transmission and supercontinuum generation in holey fiber using a diode pumped Ytterbium fiber source," Opt. Express **10**, 382–387 (2002); http://www.opticsexpress.org/abstract.cfm?URI=OPEX-10-8-382
3. T. A. Birks, W. J. Wadsworth, P. St. J. Russell, " Supercontinuum generation in tapered fibres," Opt. Lett. **25**, 1415-1417 (2000).
4. A. V. Husakou and J. Hermann, "Supercontinuum Generation of Higher Order Solitons by Fission in Photonic Crystal Fibers," Phys. Rev. Lett. **87**, 203901 (2001).
5. J. Herrmann, U. Griebner, N. Zhavoronkov, A. Husakou, D. Nickel, J. C. Knight, W. J. Wadsworth, P. St. J. Russell, G. Korn,"Experimental Evidence for Supercontinuum Generation by Fission of Higher-Order Solitons in Photonic Fibers," Phys. Rev. Lett. **88**, 173901 (2002).
6. J. M. Dudley, L. Provino, N. Grossard, H. Maillotte, R. S. Windeler, B. J. Eggleton, S. Coen, " Supercontinuum generation in air-silica microstructured fibers with nanosecond and femtosecond pulse pumping," J. Opt. Soc. Am. B **19**, 765-771 (2002).
7. A. Gaeta, "Nonlinear propagation and continuum generation in microstructured optical fibers," Opt. Lett. **27**, 924-926 (2002).
8. J. M. Dudley and S. Coen, "Coherence properties of supercontinuum spectra generated in photonic crystal and tapered optical fibers," Opt. Lett. **27**, 1180-1182 (2002).

#1473 - $15.00 US Received July 17, 2002; Revised October 15, 2002

9. M. N. Islam, G. Sucha, I. Bar-Joseph, M. Wegener, J. P. Gordon, D. S. Chemla, "Femtosecond distributed soliton spectrum in fibers," J. Opt. Soc. Am. B **6**, 1149-1166 (1989).
10. P. K. A. Wai, C. R. Menyuk, Y. C. Lee, H. H. Chen, "Nonlinear pulse propagation in the neighborhood of the zero-dispersion wavelength of monomode optical fibers," Opt. Lett. **11**, 464-466 (1986).
11. G. P. Agrawal, *Nonlinear Fiber Optics*, Academic Press, Second Edition (2001).
12. B. R. Washburn, S. E. Ralph, P. A. Lacourt, J. M. Dudley, W. T. Rhodes, R. S. Windeler, S. Coen, "Tunable near-infrared femtosecond soliton generation in photonic crystal fibers," Electron. Lett. **37**, 1510-1512 (2001).
13. L. Xu, X. Gu, M. Kimmel, P. O'Shea, R. Trebino, A. Galvanauskas, " Ultra-broadband IR continuum generation and its phase measurement using cross-correlation FROG," Paper CTuN1, Conference on Lasers and Electro-Optics (CLEO), Opt. Soc. America (2001).
14. X. Gu, L. Xu, M. Kimmel, E. Zeek, P. O'Shea, A. P. Shreenath, R. Trebino, R. S. Windeler, "Frequency-resolved optical gating and single-shot spectral measurements reveal fine structure in microstructure fiber continuum, Opt. Lett. **27**, 1174-1176 (2002).
15. K. J. Blow, D. Wood, "Theoretical description of transient stimulated Raman scattering in optical fibers," IEEE J. Quant. Electron. **25**, 2665-2673 (1989).
16. S. Coen, A. H. L. Chau, R. Leonhardt, J. D. Harvey, J. C. Knight, W. J. Wadsworth, and P. St. J. Russell, "White light supercontinuum generation with 60-ps pump pulses in a photonic crystal fiber," Opt. Lett. **26**, 1356-1358 (2001).

## 1. Introduction

The generation of ultrabroadband supercontinuum (SC) spectra has now been demonstrated by several groups by injecting high power pulses near the zero dispersion wavelength of photonic crystal fibers (PCF) [1,2]. Similar broadband SC have also been observed in standard optical fiber tapered to a strand diameter ~2 μm where the tapering introduces dispersion and nonlinearity characteristics similar to those of PCF [3]. Numerical simulations of such SC generation have also recently been reported, leading to an improved understanding of the underlying spectral broadening mechanisms involved [4–8]. In particular, for SC generated with femtosecond pulse pumping, the dominant contribution to the long wavelength extension of the SC has been shown to be associated with soliton break up combined with the Raman self-frequency shift [9] whilst an important contribution to the short-wavelength portion of the SC is due to the associated transfer of energy into the normal dispersion regime via the generation of non-solitonic dispersive wave radiation [10].

Although these spectral broadening mechanisms have, of course, been the subject of much previous research in nonlinear fiber optics over many years [11], the enhanced nonlinear response of PCFs permits their study in a regime not readily accessible with standard optical fibers. At the same time, however, it also leads to difficulties in accurately characterizing the complex temporal and spectral structure of the SC, and this has limited comparisons between theory and experiment to only relatively simple studies of the spectral properties via the positions of the observed Raman soliton peaks [5,12].

Recently, however, cross-correlation frequency resolved optical gating (XFROG) has been applied to SC characterization, permitting the first complete intensity and phase characterisation of SC generated in PCF [13,14]. The results have shown very complex time-frequency domain characteristics, and the purpose of this paper is to use numerical simulations based on an extended nonlinear Schrödinger equation (NLSE) to aid in the interpretation of these measurements. In addition, the simulations show that the time-frequency distribution afforded by the XFROG trace provides a particularly useful representation for characterizing the complex temporal and spectral evolution associated with SC generation, and an intuitive means of interpreting correlated temporal and spectral SC features. We compare our simulations with a typical experimental XFROG measurement of a generated SC, and show very good qualitative agreement.

## 2. Numerical Simulations

The simulations are based on an extended NLSE which is valid approximately down to the three optical cycle regime, and includes higher order nonlinearity and stimulated Raman

#1473 - $15.00 US Received July 17, 2002; Revised October 15, 2002

scattering [15]. The fiber dispersion was included over the range 300–1600 nm, and we note that the use of this model has previously proven successful in describing many features of SC generation in PCF [6,12,16]. For the results considered here, propagation was simulated for a 15 cm length of large air-fill fraction microstructure fiber with a zero dispersion wavelength (ZDW) at 780 nm. Figure 1 presents simulation results showing the spectral and temporal evolution as a function of propagation distance for 30 fs FWHM, 10 kW peak power input pulses injected at 800 nm.

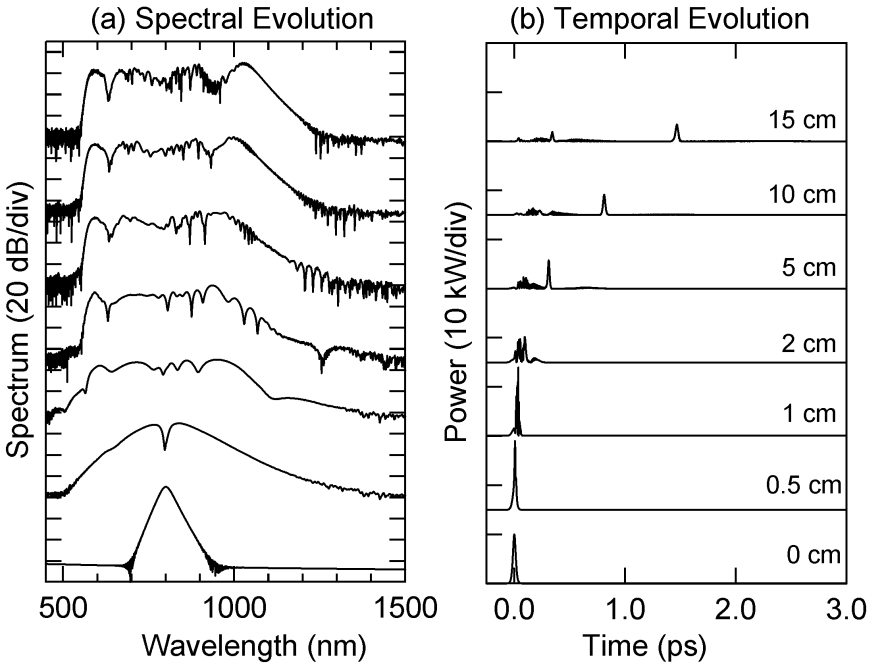


Fig. 1. (a) Spectral and (b) temporal evolution in microstructure fiber of an injected 10kW peak power 30 fs input pulse injected at 800 nm.

The initial propagation is dominated by strong temporal compression and approximately symmetrical spectral broadening, but after ~2 cm, the broadening becomes strongly asymmetric and is associated with the development of complex temporal features. In particular, the figure shows temporal pulse break-up, the development of ultrafast temporal oscillations on portions of the temporal intensity profile, as well as the generation of distinct soliton pulses in the anomalous dispersion regime which separate from the residual input pulse due to group velocity walk-off. With further propagation, these solitons undergo a continuous shift to longer wavelengths due to the Raman self-frequency shift, leading to increased spectral broadening which extends over an octave at the –20 dB level from 550–1100 nm at the output.

Figure 2 shows the output characteristics in more detail, with numerical filtering used to relate the distinct Raman solitons labeled A and B with the corresponding peaks in the output spectrum. The figure also shows several other interesting features. For example, a portion of the output temporal intensity profile is shown on an expanded timebase in order to highlight the ultrafast oscillations which have developed during propagation. The oscillation frequency varies across the profile, with the mean frequency estimated at 115 THz. Another feature of interest is the strong normal dispersion-regime peak labelled DW around 600 nm on the spectrum. This peak arises from the resonant transfer of energy from the Raman solitons via

#1473 - $15.00 US Received July 17, 2002; Revised October 15, 2002

dispersive wave generation, and is manifested in the time-domain as a broad low-amplitude pulse on the soliton trailing edge [10].

In this regard, we note that, although Raman effects play an important role in the later stages of the SC generation, the proximity of the input wavelength to the fiber ZDW means that the initial propagation is dominated by the interaction of self-phase modulation and self-steepening with higher-order dispersion (particularly third order dispersion). Indeed, numerical simulations which have been carried out with the Raman gain term set to zero have clarified that the Raman contribution to the nonlinearity is not the fundamental mechanism underlying the initial emergence of the anomalous dispersion regime soliton peaks. Rather, this is due to soliton fission effects which are seeded by ultrafast modulation instability on the pulse envelope [4-8]. However, although distinct anomalous dispersion regime solitons (and the associated normal dispersion regime dispersive wave peaks) can be observed in simulations carried out with zero Raman gain, the generated solitons clearly do not undergo the self-frequency shift to longer wavelengths with propagation, and thus the overall spectral width of the SC which is generated at the fiber output is substantially reduced.

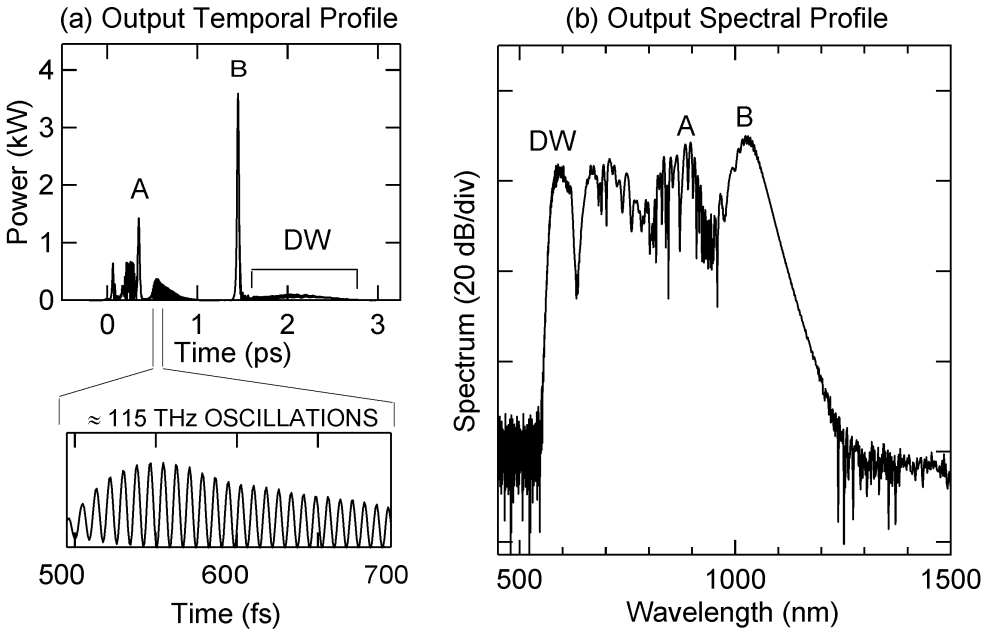


Fig. 2. Detailed view of output (a) temporal and (b) spectral characteristics.

The spectral characteristics shown in Fig. 2 are in good agreement with previous experimental studies of SC generation, which have reported strong normal dispersion regime peaks and distinct Raman soliton formation [2, 6]. Although numerical filtering is useful in correlating related temporal and spectral features of the continuum, these related features are seen more directly in the corresponding XFROG trace of the fiber output. To this end, Fig. 3 plots the XFROG trace calculated from the spectral resolution of the sum-frequency generation (SFG) intensity cross-correlation between the generated SC output and the 30 fs input pulse at 800 nm. The structure of the XFROG trace is compared with the SC temporal intensity (bottom) and spectrum (right) and we note that the spectral plot uses a nonlinear wavelength axis so that structure in the XFROG trace at a particular SFG wavelength can be directly related to the corresponding SC spectral component.

#1473 - $15.00 US Received July 17, 2002; Revised October 15, 2002

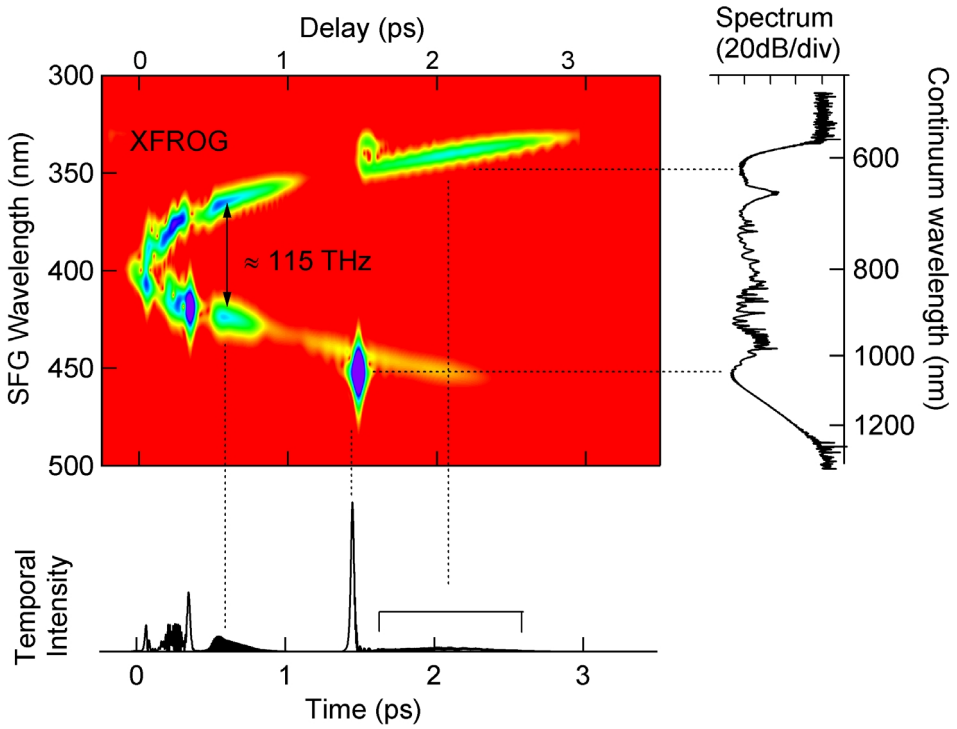


Fig. 3. (917 KB) Calculated XFROG trace with its structure correlated with the intensity and spectrum showing evolution with propagation distance. Note the nonlinear wavelength axis used in the plot of the fundamental SC spectrum.

The advantages of using a time-frequency XFROG measurement for interpreting the different SC features can be clearly seen from this figure. For example, the simple visual inspection of the XFROG trace allows the particular time and frequency domain signatures of the dispersive wave and Raman soliton components to be immediately identified and correlated. In addition, the parabolic group delay variation with wavelength (related to the dispersive characteristics of the fiber) is immediately apparent. Even more significantly, since the portion of the temporal intensity profile which has developed ultrafast oscillations is seen to be associated with two distinct XFROG wavelength components separated by 115 THz, the origin of the ultrafast modulation can be physically interpreted as a result of the beating between these components. (Note that differences between frequencies in the fundamental SC spectrum and their corresponding XFROG components are identical.) Significantly, the XFROG trace allows the origin of this modulation to be readily identified in a way which is not possible from examining the separate intensity and spectral measurements.

For the purposes of developing an intuitive appreciation of XFROG measurements of SC generation, we have found it very instructive to animate the evolution of the temporal intensity, spectrum and XFROG trace as a function of propagation distance in the fiber. A link to such an animation is given in the caption to Fig. 3, and it is clear that this clearly shows how the onset of pulse break up and the formation of Raman solitons is associated with the development of distinct peaks in the spectrum and, in addition, how the associated generation of the dispersive wave occurs at increasingly shorter wavelengths as the Raman soliton shifts to longer wavelengths. More generally, we find that viewing pulse propagation in optical fibers in the time-frequency domain allows the evolution of the pulse properties to be seen in a way which is not possible with separate time and frequency domain representations such as shown in Fig. 1.

#1473 - $15.00 US
Received July 17, 2002; Revised October 15, 2002

## 3. Qualitative Comparison with Experiment

Several experiments have now reported preliminary XFROG measurements to characterize the intensity and phase of ultrabroadband SC spectra [13, 14] and in this section we compare the qualitative characteristics of a typical experimental XFROG measurement with the simulation results described above. Although uncertainties in the fiber parameters used in the experiments preclude a detailed quantitative comparison with simulations, the numerical results above nonetheless allow several distinct features seen in the experimental XFROG traces to be physically interpreted.

The experiments involved generating a supercontinuum in a 16 cm length of microstructure fiber using a 100 MHz train of 25 fs pulses at 800 nm with energy around 1 nJ. For the XFROG measurement, the fiber output was gated by the 800 nm pump pulse in a 1 mm thick BBO crystal, which was rapidly angle-dithered with an amplitude of about 20°. Angle-dithering the crystal allowed for phase-matching at all wavelengths in the continuum. The delay between the continuum and gate pulses was scanned in 33-fs steps (shorter time resolution than 33 fs is obtained due to the large spectral range used in the measurements), and the sum-frequency signal pulse generated by the continuum and gate beams was spectrally resolved at each delay, forming a 370×1024 trace, which was further interpolated into a 4096×4096 trace for retrieval of the intensity and phase (required to satisfy the discrete Fourier transform relations for a pulse with such a large time-bandwidth product). The supercontinuum intensity and phase vs time and frequency were retrieved using the commercial Femtosoft XFROG software.

Figure 4 shows the experimental results. The measured and retrieved XFROG traces are in excellent qualitative agreement, with the additional fine structure observed in the retrieved trace due to shot-to-shot instability of spectral fine structure in the continuum spectrum. This unstable fine structure is interesting and has been discussed in detail in [14], but is not relevant to the discussion here of the large-scale structure. As in Fig. 3, we have plotted the retrieved temporal intensity and spectrum beside the measured XFROG trace and have identified several spectral and temporal features that correspond to features in the measured trace. Like the simulations, the retrieved intensity exhibits a low amplitude oscillatory structure associated with distinct XFROG wavelength components. We have exploded part of this structure in the figure to illustrate that, despite their low amplitude, these oscillations are well recovered by the XFROG measurement and retrieval. The mean oscillation period is around 8.8 fs, consistent with the 114 THz period between the corresponding temporally coincident components in the XFROG trace. This is, we believe, the first experimental evidence of this predicted ultrafast oscillatory structure in SC generation in microstructure fiber.

#1473 - $15.00 US Received July 17, 2002; Revised October 15, 2002

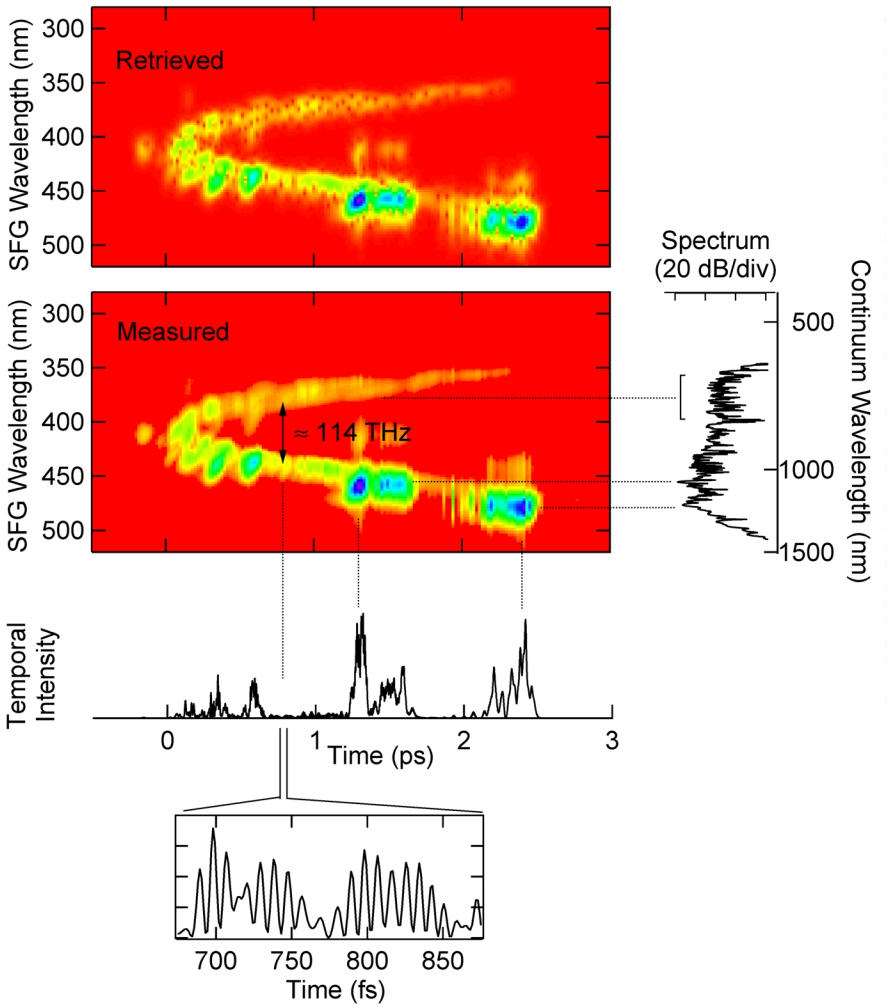


Fig. 4. Measured and Retrieved XFROG traces with the structure of the measured trace correlated with the retrieved intensity and spectrum. Note the nonlinear wavelength axis used in the plot of the fundamental SC spectrum. The exploded view illustrates the low amplitude oscillations in the retrieved intensity.

## 4. Conclusions

Analyzing SC generation via the XFROG trace allows related spectral and temporal features to be intuitively correlated and permits their physical origin to be readily identified, despite their considerable complexity. The numerical simulations described here based on a generalized NLSE predict distinct features such as Raman soliton and ultrafast envelope oscillations which have also been confirmed using experiments. More generally, we believe that we have shown the advantages of using a visual time-frequency approach for the analysis of the complex spectral and temporal structure of SC generation.

#1473 - $15.00 US
Received July 17, 2002; Revised October 15, 2002